Global and Regional Hydrological Impacts of Global Forest Expansion

James A. King[*1,3], James Weber[1, 3], Peter Lawrence[2], Stephanie Roe[4], Abigail L. S. Swann[5],

and Maria Val Martin[1, 3]

1 – School of Biosciences, University of Sheffield, UK

2 – Terrestrial Sciences Section, National Center for Atmospheric Research, Boulder, CO, USA

3 – Leverhulme Centre for Climate Change Mitigation, School of Biosciences, University of Sheffield, UK

4 – World Wildlife Fund, Washington, DC, USA

5 - Department of Atmospheric Science and Department of Biology, University of Washington, Seattle, WA, USA

* Author to whom correspondence should be addressed - james.king@sheffield.ac.uk.

Abstract

Large-scale reforestation, afforestation, and forest restoration schemes have gained global support as climate change mitigation strategies due to their significant carbon dioxide removal (CDR) potential. However, there has been limited research into the unintended consequences of forestation from a biophysical perspective. In the Community Earth System Model version 2 (CESM2), we apply a global forestation scenario, within a Paris Agreement-compatible warming scenario to investigate the land surface and hydroclimate response. Compared to a control scenario where land use is fixed to present-day levels, the forestation scenario is up to 2°C cooler at low latitudes by 2100, driven by a 10% increase in evaporative cooling in forested areas. However, afforested areas where grassland or shrubland are replaced lead to a doubling of plant water demand in some tropical regions, causing significant decreases in soil moisture (~5% globally, 5-10% regionally) and water availability (~10% globally, 10-15% regionally) in regions with increased forest cover. While there are some increases in low cloud and seasonal precipitation over the expanded tropical forests, with enhanced negative cloud radiative forcing, the impacts on large-scale precipitation and atmospheric circulation are limited. This contrasts with the precipitation response to simulated large-scale deforestation found in previous studies. The forestation scenario demonstrates local cooling benefits without major disruption to global hydrodynamics beyond those already projected to result from climate change, in addition to the cooling associated with CDR. However, the water demands of extensive forestation, especially afforestation, have implications for its viability given uncertainty in future precipitation changes.

1. Introduction

The need to achieve net zero carbon emissions in order to reach the Paris Agreement climate targets demonstrates the importance of drastic emission reductions as well as effective carbon dioxide (CO_2) removal (CDR) (Fankhauser et al., 2021). Enhancing the capacity of the terrestrial biosphere to absorb and store CO_2, including through afforestation (planting trees on previously unforested land), reforestation (planting trees on previously forested land), and forest restoration (repairing degraded forests), has emerged an important strategy for climate change mitigation. (Girardin et al., 2021; IPCC, 2022; Roe et al., 2021). Indeed, the full realisation of countries' Paris Agreement commitments would result in forests absorbing 1.1 ± 0.5 GtCO2e yr^{-1} by 2030, representing ¼ of planned emissions reductions (Grassi et al., 2017; Smith et al., 2023). In addition to national climate commitments, countries and private sector actors have made global restoration commitments, including the Bonn Challenge and the UN Decade on Ecosystem Restoration, in which 74 countries initially agreed to restore 350 Mha of degraded land by 2030. This has since increased to 115 countries and up to 1000 Mha of land restoration by 2040 (Sewell et al., 2020). A wide range of private sector and non-governmental land and forest restoration commitments, as well as tree planting initiatives, have also been launched in recent years (Martin et al., 2021, Seddon et al., 2021).

CDR potential as it relates to climate change mitigation potential is generally estimated by calculating the amount of carbon sequestered from the atmosphere by a given intervention compared to a counterfactual scenario without the intervention. Several recent studies have attempted to quantify the CDR potential of global-scale reforestation, afforestation, and forest restoration, with variable estimates resulting from

different methodological approaches (e.g. Griscom et al., 2017, Roe et al., 2019, Seddon et al., 2021).
For example, Bastin et al., (2019) suggested that an additional 900 Mha of tree cover could potentially exist with an additional storage capacity of 205 PgC, although the magnitude of this CDR potential was argued to be several times overestimated (Friedlingstein et al., 2019; Lewis et al., 2019a). Lewis et al. (2019b) gave an estimate of 1200 Mha of suitable land area for restoring natural forest ecosystems, while estimating a maximum storage capacity of 42 PgC by 2100 for the initially committed Bonn Challenge land area if it is entirely given over to forest restoration (144 PgC for the maximum possible area). Griscom et al. (2017) found that estimates of potential reforestation area ranged from 345-1779 Mha and defined their own 678 Mha 'area of opportunity' for the regrowth of natural forests. Cook-Patton et al. (2020) used this area to derive a maximum biosphere CDR potential of 2.43 PgC yr^{-1} by 2050.

Beyond carbon sequestration, it is also important to estimate the broader climate impacts of large-scale forest expansion (Seddon et al., 2020). Forests influence climate in complex ways and at multiple spatial scales (Bonan, 2008, 2016), which can broadly be categorised into biogeophysical and biogeochemical. Biogeophysical impacts result from changes to the surface energy balance. These include the effect of the reduced albedo of trees when compared to other land cover types, such as cropland or grassland (Kirschbaum et al., 2011; Windisch et al., 2021). The albedo effect is particularly pronounced for expansion of forests over previously snow-covered tundra landscapes (De Wit et al., 2014; Bonan et al., 1992), which reduces the climate mitigation potential of forest expansion in high latitude regions such as Northern Canada (Drever et al., 2021). Other less well understood biogeophysical impacts include changes to soil moisture and evapotranspiration (Nosetto et al., 2005), which can affect both temperature (through changes to surface energy balance; Barnes et al., 2024) and rainfall (through changes to cloud cover; Duveiller et al., 2021). Locally, this can have both positive and negative impacts on extreme weather events (Abiodun et al., 2013). At continental and hemispheric scales, increased moisture availability can drive changes to latent heating that affect remote atmospheric dynamics (Laguë et al., 2021) including the general circulation of the atmosphere (Portmann et al., 2022). Increased soil water demand from the land use change from grassland or cropland to forest has implications for water supply to both forests themselves and nearby communities (Hoek van Dijke et al., 2022). Biogeochemical impacts of forest expansion beyond carbon sequestration derive from increased emissions of biogenic volatile organic compounds (BVOCs) such as isoprene (Bonan, 2008; Šimpraga et al., 2019). BVOCs undergo complex chemical reactions in the troposphere, including oxidation to form secondary organic aerosols (SOA) (Sporre et al., 2019; Zhang et al., 2023) as well as affecting air quality with implications for human health (Heald and Spracklen, 2015; Val Martin et al., 2015) and food security (Tai et al., 2014). The chemical processes which BVOCs undergo in the atmosphere affect tropospheric concentrations of the greenhouse gases CH_4 and O_3, organic aerosols, and cloud properties, with radiative impacts which, when combined with albedo, may offset up to a third of the climate mitigation benefits from forest-based CDR depending on the level of future warming (Weber et al., 2024; Zhang et al., 2023). In this analysis we focus on the biogeophysical and hydrological impacts on the land surface and clouds, while noting that BVOC chemistry and hydrology are not separable because of the impact of the former on radiative forcing, cloud nucleation, and other important processes.

While there is a substantial literature on the interactions between forests and climate (Bonan, 2016), which increasingly incorporates recent advances in satellite-based remote sensing and Earth System modelling, there has been less attention given to evaluating the consequences of forest-based CDR strategies beyond attempts to quantify their carbon sequestration potential, despite the prominence of these strategies in the policy sphere. Recent advances have been made from observations of forest cover change affecting low-level clouds (Duveiller et al., 2021), or from the application of idealised forest cover scenarios to identify changes in atmospheric circulation (Portmann et al., 2022). There has also been

120   much recent attention given to the climate impacts of deforestation (e.g. Alkama & Cescatti, 2016; Bekenshtein et al., 2023; Boysen et al., 2020; Lawrence et al., 2022; Lee et al., 2023; Smith et al., 2023; Swann et al., 2015a), but it is not clear if the processes by which deforestation affects climate are reversable in the case of deliberate increases in forest cover. There is therefore a need to evaluate and estimate the broader climate impacts from plausible forestation proposals in the context of climate change

125   mitigation (Fuhrman et al., 2020; Orlov et al., 2023; Zickfeld et al., 2023), in particular reflecting the necessity that such mitigation is just (Robinson and Shine, 2018; Fleischman et al., 2020) and avoids placing a mitigation burden on the Global South in response to emissions from the Global North (Bond et al., 2019; Parr et al., 2024). In this study, we use an Earth System Modelling framework to investigate the impacts of large-scale forest expansion on the water cycle. We first assess how such a global-scale

130   scenario influences key processes at the land surface; secondly, we examine the potential meaningful effects on cloud cover, precipitation and atmospheric circulation.

2. Methods

135   Investigating global forest-climate interactions necessitates the use of a fully coupled Earth System Model (ESM) which simulates feedbacks between the terrestrial biosphere, atmosphere, and oceans. We use version 2.1.3 of the Community Earth System Model (CESM2; Danabasoglu et al., 2020) at 0.9° x 1.25° horizontal resolution. The atmospheric component is the Community Atmosphere Model version 6 with the MOZART Troposphere/Stratosphere (TS1) chemistry mechanism (CAM6-Chem; Emmons et al.,

140   2020) and the 4-mode version of the Modal Aerosol Model (MAM4; Liu et al., 2016). The model has a 32-layer atmosphere extending to ~ 3hPa, with prescribed stratospheric aerosols above the model top. The land model is the Community Land Model version 5 (CLM5; Lawrence et al., 2019) with prognostic vegetation and fully active biogeochemistry, which incorporates the Model of Emissions and Gases from Nature version 2.1 (MEGAN2.1; Guenther et al., 2012). The ocean model used is the Parallel Ocean

145   Program version 2 (POP2; Danabasoglu et al., 2012). The model configuration employed is similar to that used in the CESM2 contribution to ScenarioMIP, but with the addition of a prognostic atmospheric chemistry scheme.

To evaluate the impacts of global-scale forestation, we performed three sets of model experiments which

150   differed only in the prescribed land use and land cover change (LULCC). All experiments were forced using prescribed well-mixed greenhouse gases (WMGHGs, such as CO_2, CH_4, and N_2O) as fixed lower boundary conditions following the SSP1-2.6 scenario. This scenario is consistent with the Paris Agreement targets as it results in a global mean surface temperature increase by 2100 relative to pre-industrial conditions of ~1.7°C (Gidden et al., 2019). We use this emissions scenario because we assume

155   that a world in which large-scale forest expansion is implemented is a world in which climate change mitigation is prioritised, and where Paris-compatible measures on emissions reduction are also implemented. We also prescribe SSP1-2.6 non-GHG anthropogenic emissions (for example from biomass burning, aircraft, and shipping). Anthropogenic emissions derive from the Community Emissions Data System (CEDS; Hoesly et al., 2018) and biomass burning from Input4MIPs (Gidden et al., 2019).

160   Biogenic emissions are actively simulated by MEGAN. We do not consider the role of fire in this study as we aim here to isolate hydrological impacts directly caused by forest expansion, rather than from second-order feedbacks that may obscure the direct signals. Therefore, there is no active fire model used.

The control experiment (SSP1-2.6 without LULCC, or 'No LULCC') follows SSP1-2.6 GHGs and anthropogenic emissions, but LULC data are fixed at 2015 levels based on the incorporation into CLM5

165   of historical data from the Land Use Harmonised transient dataset version 2 (LUH2; Lawrence et al., 2016). In this setup, the biosphere can respond to changes in climate and CO_2 fertilisation through photosynthesis and LAI, for example, but the proportion of each grid cell covered by each land use type is fixed. The next set of experiments (SSP1-2.6, or 'Base') followed the SSP1-2.6 LULCC trajectory from ScenarioMIP. This represents a well-established reference point for a Paris-compatible future and

170   serves as a moderate reforestation scenario in which tree cover increases globally by 10% by 2100 compared to 2015, but there is also some deforestation and expansion of agricultural land at a regional level.

The experiment with large-scale forestation (SSP1-2.6 Max Forest, or 'Max Forest') used a scenario developed by Roe et al. (2021) within CLM5, and also used in Weber et al. (2024), to evaluate the

175   climate change mitigation potential of reforestation (of rangeland, secondary forest and secondary non-forest in forest biomes), afforestation (of rangeland, secondary forest and secondary non-forest in non-forest biomes where tree cover is greater than 10%), and forest enhancement (of forests where tree cover density is less than its potential). This scenario achieves an average rate of CDR under SSP1-2.6 GHG forcing of 5.1 GtCO$_2$ yr^{-1} by 2050 (Roe et al., 2021), which is within the ranges found in previous studies

180   (Lawrence et al., 2018; Nabuurs et al., 2023). We define the 'Max Forest' scenario using the maximum values of all three forest expansion strategies evaluated by Roe et al. (2021). The scenario operates by expanding areas of existing forest cover into suitable area as defined by a bioclimatic envelope approach (Whittaker, 1975). This avoids planting trees in areas where they would be unlikely to grow, such as arid environments; it also ensures a realistic distribution of plant functional types (PFTs) suitable for each

185   biome. This approach has the additional benefit of limiting high-latitude tree growth in existing tundra environments while concentrating forest expansion at the margins of tropical rainforests (Fig. 1), aiming to minimise the enhanced local warming associated with albedo decrease in cold tundras while maximising the local evaporative cooling associated with tropical rainforests (Roe et al., 2021). The scenario also excludes forestation in IUCN designated protected areas in an effort to limit potential negative impacts

190   on existing biodiversity and ecosystem structure and function; there is substantial overlap (42%) between areas of forest restoration in this scenario and priority areas for biodiversity conservation and ecosystem service provision under the 'Sharing the Planet' scenario (Kok et al., 2023). Food security concerns around forest expansion are addressed by fixing agricultural areas at 2015 levels and preventing forest from encroaching upon them. The Max Forest scenario thus presents a biophysical maximum for forest

195   expansion in the 21st century which considers global priorities around biodiversity and food security as well as climate change. In addition, Max Forest is comparable to existing ambitious targets for land restoration, including the Bonn Challenge targets, as well as current global restoration commitments ('GRC') – although the latter also include non-forest restoration (Sewell et al., 2020) (Fig. S1). We select 6 main regional domains (North America, Europe, Amazon, Congo, South and East Asia, and the

200   Southern Cone; Fig. 1A) as they represent areas with large tree cover, and show results for the globe alongside the Congo Basin, and Amazon, as these tropical rainforest basins are global priorities for forest restoration. Detail on other domains is provided in the Supplementary Information.

In order to account for the process of model internal variability arising from the use of a fully coupled land-ocean-atmosphere experimental setup, three ensemble members were run for each experiment

205   using varying initial conditions for 2015 taken from the endpoint of different historical runs of CESM2 from ScenarioMIP. This approach provided us with initial conditions which were 'spun-up', but also represented a reasonable sample of the uncertainty associated with simulating the present-day state of the Earth system. The analysis presented here refers to the ensemble means for each experiment. Each ensemble member was run from 2015-2100 to control for internal climate variability, such as ENSO, we

take decadal mean values from 2015-2025 to represent '2020', 2045-2055 for '2050', and 2090-2100 for '2095' in the analysis.
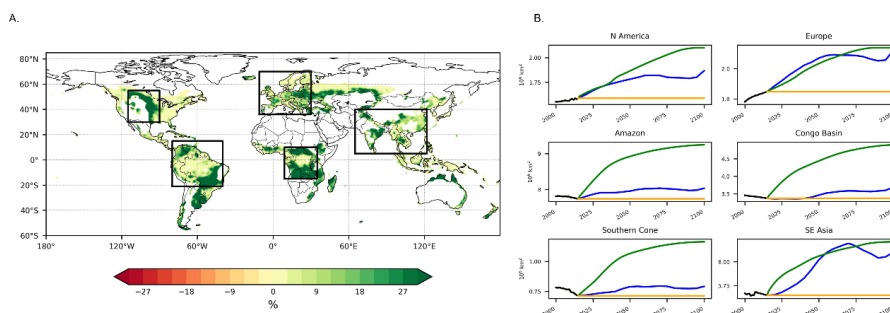
Figure 1 – *The Max Forest scenario in the context of the Shared Socioeconomic Pathways (SSPs). A – percentage increase in forest cover, 2095 minus 2015, with boxes showing the different regional domains. B - Regional changes in total forest area for the Base (blue), Max Forest (green), and No LULCC (orange) experiments. Historical data from LUH2 for 2000-2014 are shown in black.*

3. Results

3.1. Changes to Land Surface Processes

Figure 2 shows the effect of forestation on near-surface temperatures. In the Max Forest scenario, near-surface air temperatures in forested areas are on a global average 0.48°C cooler than the No LULCC and 0.38°C cooler than Base by the end of the 21ˢᵗ century. Zonally averaged tropical near-surface air temperatures in the northern (southern) tropics are up to 0.55°C (0.75°C) cooler in Max Forest compared to No LULCC in 2095 (Fig. 2A). Fig. 2 demonstrates that the Max Forest scenario effectively removes the global warming signal from the Congo Basin domain, as there is effectively no warming at 2050 or 2095 relative to 2015 and a small but significant cooling (~2%) over the areas where forest cover increases most (Fig. 2B). The Max Forest scenario is also significantly cooler in the most forested parts of the Amazon than both SSP1 Base and No LULCC at 2050 and 2095 (Fig. 2B). The Max Forest scenario is up to 2°C cooler than in the No LULCC scenario at the margins of tropical rainforest basins, in particular central Africa, southern Brazil, Colombia and Venezuela, and northern Australia, which are key targets for forest expansion in the scenario. It is important to note that GHG concentrations were prescribed following SSP1-2.6 in our experiments. Consequently, the cooling effect due to CDR is purely biophysical and not due to any change in the atmospheric concentration of CO_2. Fig. 2A shows some near-surface warming in the central USA and the Russian/Kazakh border which is driven by local albedo decreases (Fig. S2). The North America domain is ~0.2°C warmer at the end of the 21ˢᵗ century in Max Forest compared to No LULCC. However, this temperature difference is not statistically significant at the 95% confidence level (Fig. 2A). Much of the northern hemisphere midlatitudes are cooler in Base than in the Max Forest scenario; as the greatest temperature differences between the scenarios are located

over the Canadian Arctic where neither scenario changes forest cover. This effect may be related to SST biases in the Labrador Sea in CESM2 (Danabasoglu et al., 2020).
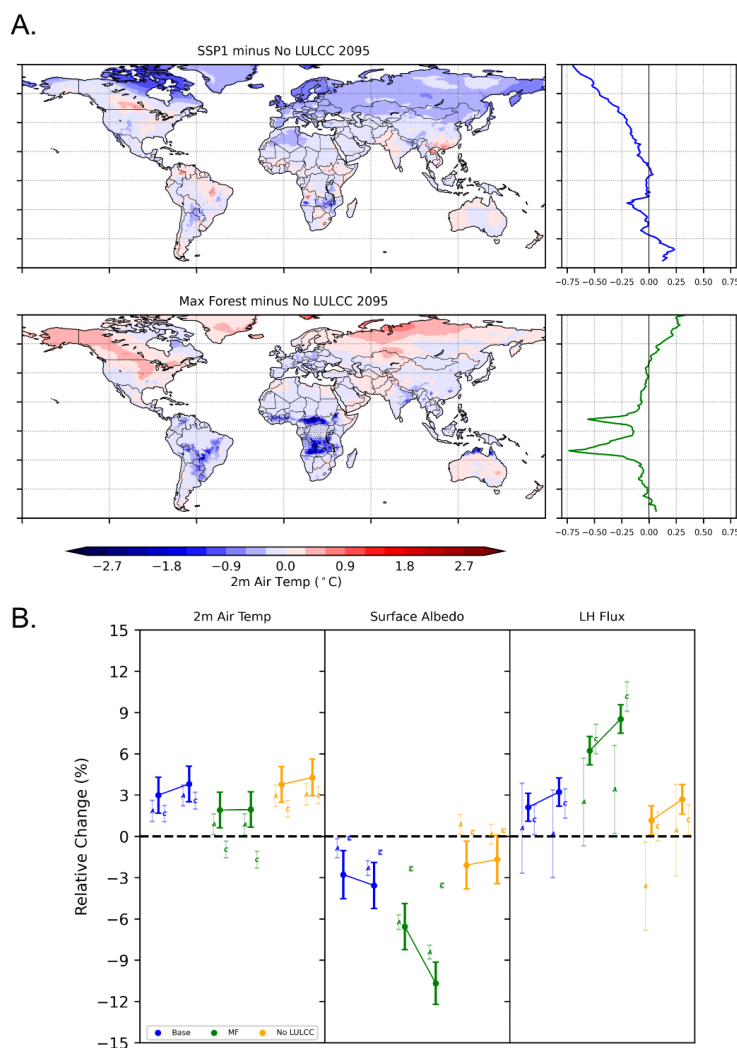
Figure 2 – *Air temperature at 2m above the land surface. A- global changes at 2095 between Base (top) and Max Forest (bottom) and No LULCC. Stippling denotes statistical significance of differences assessed using a two-tailed Student's T test at α=0.05; zonal means of the differences shown at right. B – area-weighted mean values for 2m air temperature, surface albedo, and latent heat flux, for grid cells where the increase in tree cover between 2015 and 2095 >25%, expressed as percentage differences from the 2020 mean for No LULCC. For each experiment the left point indicates the 2050 (2045-2055) mean and the right point the 2095 (2090-2100) mean. Circles indicate the global mean, 'A' the Amazon, and 'C' the Congo Basin. Error bars denote the standard error of the decadal means*
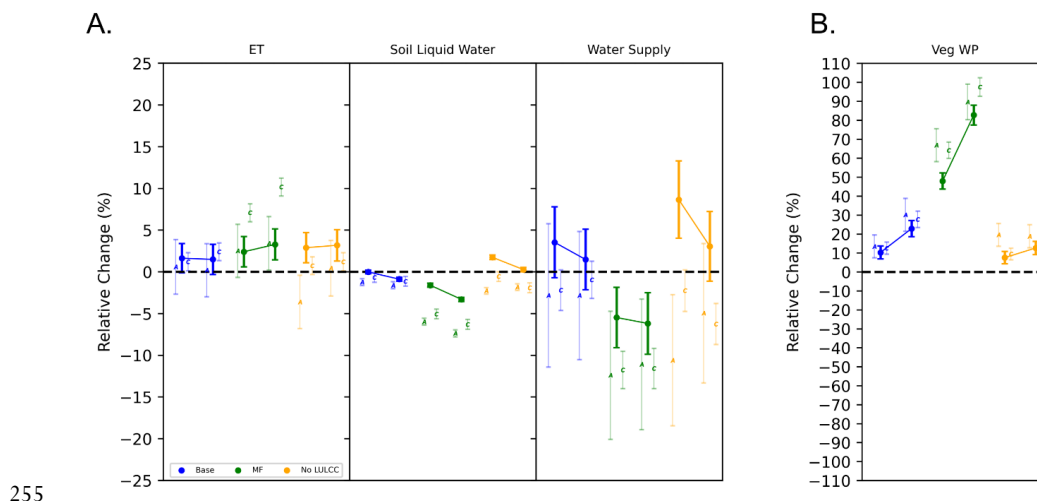
Figure 3 – As *Figure 2B, but for the annual sum of mean evapotranspiration (ET), vertically averaged soil liquid water content, water supply (runoff + river flow) (A), and vegetation water potential (B).*

Beyond affecting temperatures on global and regional scales, large-scale forestation also affects key climate-relevant processes at the land surface. In our scenario, the biosphere response to CO_2 is an upper bound, as plants take up CO_2 from the atmosphere but do not deplete it. Between 2015 and 2095 in the Congo Basin, net primary productivity (NPP) in Max Forest increases by 2.1 PgC yr^{-1} (33%) than 2015 levels while the No LULCC scenario exhibits an increase of only ~0.5 PgC yr^{-1} (Fig. S3). Increased photosynthetic activity by plants in this domain drives concurrent increases in evapotranspiration (Fig. 3). In the Congo basin, this increases by 0.2 mm day^{-1} by 2100. This increased evapotranspiration in warm, humid environments drives evaporative cooling of the surface through latent heat release (Figs.3 and 4), accounting for the reduction in surface warming seen in the tropics in Max Forest (Fig. 2).

Replacing areas of grassland or shrubland with forest can be expected to increase water demand, and consequently water stress (where demand approaches or exceeds supply) can increase if there are not corresponding increases in precipitation. This can be exacerbated under conditions of elevated CO_2 and moderate temperature increases, which can increase plant productivity if that increase in productivity outweighs water savings associated with increases in water use efficiency under elevated CO2. We use the vegetation water potential (Veg WP) as a metric for water stress in CLM5 (Kennedy et al., 2019). This quantity reflects both root and leaf hydraulics, and increasing (more negative) values reflect increases in water demand from plants as plant size increases (e.g. from grasses to trees). Stronger Veg WP increases are found in Max Forest than in the other scenarios. Globally, in Max Forest, veg WP increases by 47% in 2050 and 82% in 2095 relative to 2020 values. In contrast, the Base scenario has moderate increases of 10% in 2050 and 22% in 2095, while the No LULCC scenario exhibits an even lower increase, with 8% in 2050 and 11% in 2095 (Fig. 3). Regionally, changes in Max Forest vary from a ~66% increase in N America to a ~100% increase in tropical rainforest areas by 2095. Our results further indicate significant decreases in soil liquid water content in the Max Forest scenario in all domains apart from

Europe (Fig. 3, Fig. S6) compared to the other scenarios, which reflects a situation where plant water demand as a result of extensive forest expansion may be exceeding soil water supply across the globe. This corresponds to a global-scale decrease in surface water supply (expressed as the sum of the surface runoff and river flow) of between 5 and 10%, and between 10 and 15% in the Amazon and Congo (Fig.3)

285
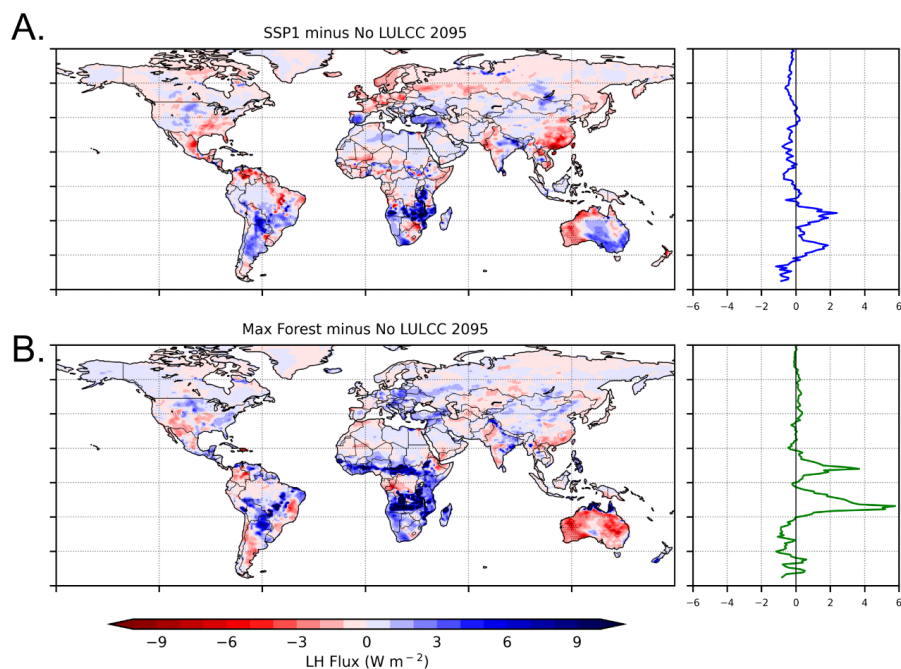
Figure 4 – *as Figure 2A but showing the differences in surface latent heat flux between experiments at the end of the 21ˢᵗ century.*

290   3.2. Changes in Cloud Cover

We assess the effects of forestation in cloud cover and related processes such as the density of cloud condensation nuclei (CCN) in Figs 5 and 6. Cloud cover is a key component of forest-climate interactions. Observational studies have found links between forest cover and convective clouds over tropical
295   rainforests (Bekenshtein et al., 2023), where evapotranspiration is a key driver of rainfall (Crowhurst et al., 2021), as well as over temperate forests where frontally-generated clouds are more common than deep convective clouds (Duveiller et al., 2021; Wang et al., 2009).

300
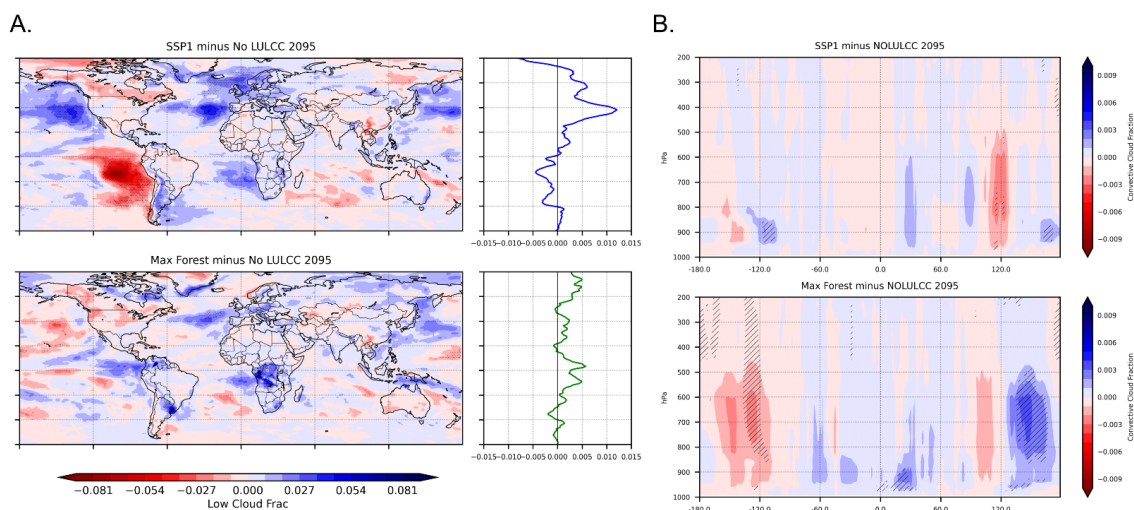
Figure 5 – *A – Differences between experiments at the end of the 21ˢᵗ century in cloud cover integrated vertically between 1200-700hPa. B – as A but showing vertical cross-sections of convective cloud cover averaged across tropical latitudes. Hatching in B denotes statistical significance of differences assessed using a two-tailed Student's T test at α=0.05.*

In tropical regions, the effects of large-scale forestation or deforestation in low latitudes are typically dominated by the impact on cloud processes (Bekenshtein et al., 2023). The tropical troposphere is frequently in a state of instability, where lifting of air masses occurs due to strong latent heating. This
305 instability drives the general circulation of the atmosphere in low latitudes through moist convection, which acts as a 'heat engine' to redistribute energy from the surface into the upper troposphere. Much of this convection is driven by evapotranspiration from tropical rainforests, though the extent to which this is true varies depending on the domain in question (Smith et al., 2023a).

In our results, we find significant increases in low cloud fraction over Argentina in Base relative to No
310 LULCC in 2095. In Max Forest, there are small but significant increases (~5%) in low-level cloud fraction (below 700hPa) over the Congo Basin, northern Australia, Uruguay, and Colombia/Venezuela in 2095 (Fig. 5A) with smaller yet significant increases of the same spatial pattern in 2050. All of these are areas with significant increases in tree cover in Max Forest. Significant differences in oceanic low cloud of both positive and negative signs are seen in both scenarios relative to No LULCC (Fig. 5A). However, given
315 the moderate nature of our land use change scenarios, attributing these changes directly to forestation is challenging. While low cloud cover is important for the surface radiation balance, changes to deep convective clouds over the tropical rainforest basins can have important consequences for regional and global climate. We find statistically significant but small (~0.2%) increases in tropical convective cloud fraction over Africa in Max Forest relative to No LULCC in 2095 (Fig. 5B) but the significant differences
320 are restricted to below 900hPa, implying a limited effect of the land use change scenario on deep convection. No significant differences at the conventional 95% confidence level were found over tropical South America and increases over the tropical Western Pacific occurred mostly in the mid-troposphere,

with commensurate decreases over the tropical Eastern Pacific implying a change to the Pacific branch of the Walker Circulation. However, the lack of corresponding changes to convective cloud over tropical
325   land suggests that this effect is not directly due to forest expansion in our scenario; Walker Circulation representation in global climate models is in any case highly uncertain (Chadwick et al., 2013; King and Washington, 2021).
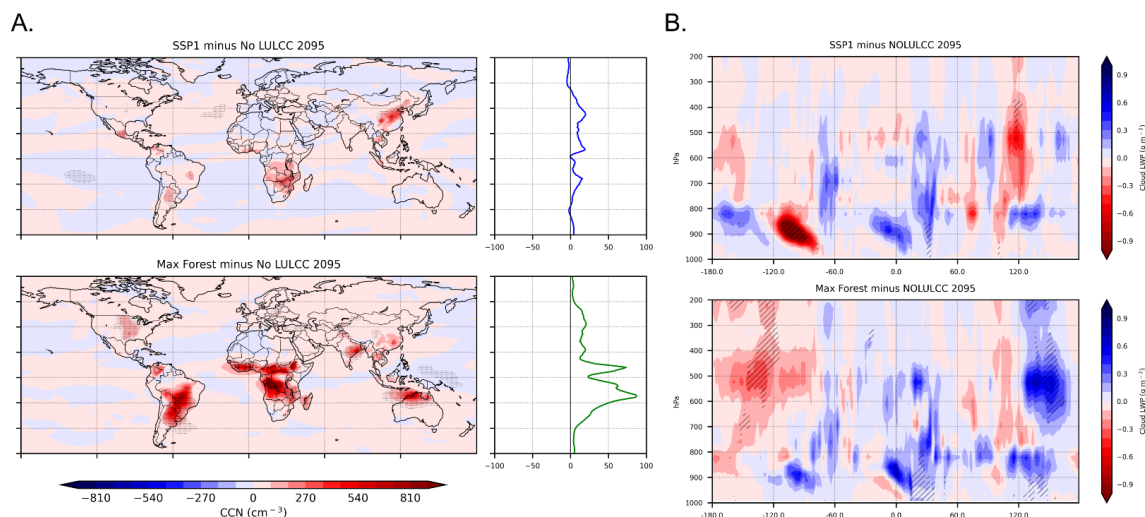
Figure 6 *– A – the vertical sum of cloud condensation nuclei (CCN) at 0.1% supersaturation, B – the total in-cloud liquid water path (LWP). Note reversed colour scale in B.*

As well as the amount of cloud cover, which is affected by evapotranspiration, forestation can also
330   influence cloud properties such as water content and the concentrations of cloud condensation nuclei (CCN). Trees provide a source of BVOCs as a by-product of a number of biological processes, and BVOC emissions are elevated during warmer conditions (Weber et al., 2022). BVOC chemistry can result in the growth and formation of secondary organic aerosols (SOA), which act as CCN. This effect can clearly be seen in Fig. 6A, where CCN concentration at 0.1% supersaturation is
335   significantly greater (up to $+1000$ cm^{-3}) over areas of increased forest cover in Max Forest at 2095 compared to No LULCC. The signal is particularly strong in the tropics due to this temperature dependence but is also significant in the central USA, implying synergies between tree type and climate in this location that are less active elsewhere in the midlatitudes (Sindelarova et al., 2014) and may be related to the expansion of deciduous forest in the US which is more emissive of isoprene
340   (Guenther et al., 2012). A similar pattern is evident when the Base scenario is compared to No LULCC. Fig. 6B shows the in-cloud liquid water path (LWP), a measure of the mass of water droplets in each model layer. There are statistically significant increases in LWP over land in tropical Africa and Australia in Max Forest compared to No LULCC, but the magnitude is small ($<$1g m^{-3}). Differences over the tropical Pacific in both SSP1 Base and Max Forest are likely a response to SST
345   pattern changes, as also observed for cloud fraction (Fig. 5). We find similar results for CCN and LWP in 2050, but with a smaller signal, in line with the changes in low cloud fraction.

The total cloud forcing, or cloud radiative effect (CRE) summarises the impact of clouds on the Earth's radiative balance and is affected by cloud fraction (i.e. cloud cover), cloud height, and cloud reflectivity (which is in turn affected by cloud water and CCN concentration). For a given scenario and time period, the CRE is calculated as the difference in net incoming top of atmosphere (TOA) radiation between a case in which clouds are included in the radiation scheme and a case where the interaction of clouds with radiation is ignored (a so-called 'clear' diagnostic). A comparison of the CRE between two scenarios or time points (e.g., SSP1 base at 2020 and 2050), termed 'forcing' here, illustrates how changes to cloud cover and cloud properties have affected the Earth's energy budget. These effects can be decomposed into SW and LW components.
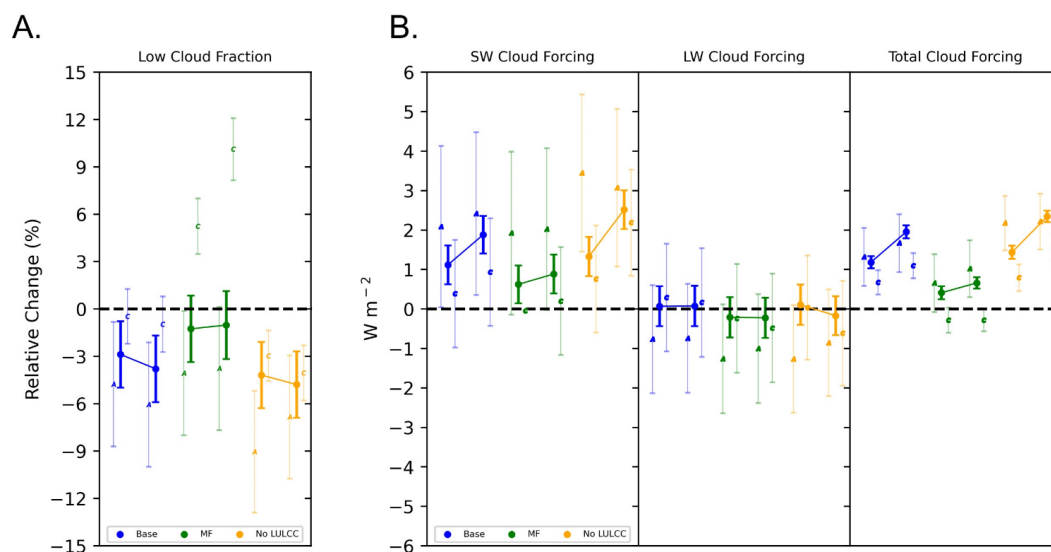
Figure 7 – *As figure 2B, but showing differences in cloud cover integrated between 1200-700 hPa (A) and differences in clean-sky shortwave cloud radiative forcing, clean-sky longwave cloud radiative forcing, and total clean-sky cloud radiative forcing (B).*

Fig. 7 shows that in the Base, Max Forest and No LULCC scenarios, the total and SW cloud forcing is positive at 2050 and 2095 relative to 2020. While clouds have a net cooling effect on the Earth in each scenario and time period, this finding indicates that the changes to clouds in 2050 and 2095 means this cooling effect is smaller than in 2020. However, this positive forcing is smaller in the Max Forest scenarios than either the Base or No LULCC, corresponding to Max Forest's smaller decrease in low cloud cover on a global scale.

Regionally, statistically significant forcings of ~-2 to -3 W m⁻² are found over parts of the Congo Basin, SE Asia, Southern Cone, as well as Northern Australia (Fig. S8). This is also consistent with a shortwave cooling effect associated with increased low cloud cover in the tropics, due to increased reflection of incoming shortwave radiation, while changes to deep convective clouds are limited in our experiments (Fig. 5B). There is also some cooling over land in Europe which is related to small

increases in shortwave cooling (Fig. S8); however, the negative CRE change here is not statistically significant.

3.3. Effects on Precipitation and Atmospheric Dynamics
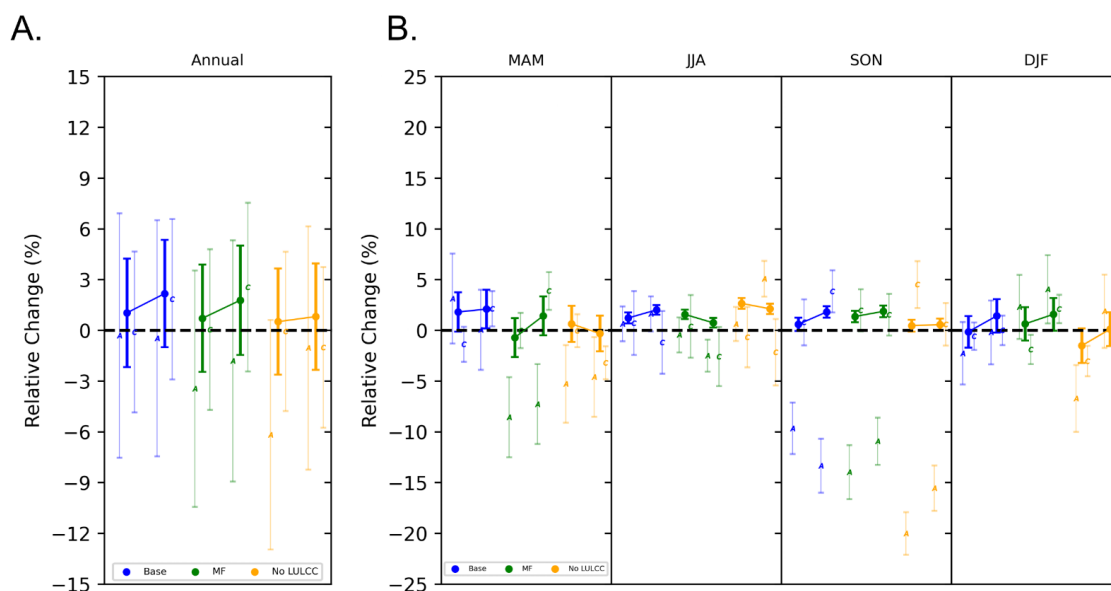
375

Figure 8 - *as Figure 2B, but showing differences in precipitation compared to 2020 between experiments in the annual mean (A) and for each meteorological season (B).*

A process chain is expected from increased latent heat flux, LWP, and cloud cover, to changes in rainfall and aspects of the general circulation (Portmann et al., 2022; Swann et al., 2012). A change in the hemispheric energy gradient resulting from forest expansion in the Northern Hemisphere, where most of the land is, drives movement of the Hadley circulation towards the warmer

380   hemisphere (Swann et al., 2012; Laguë et al., 2021). Owing to the smaller increase in forest expansion in our scenario compared with other, more idealised studies, as well as the moderate climate change scenario selected, substantial impacts on global precipitation are expected to be limited (especially given the small changes to cloud cover shown in Fig. 5). However, regional changes to precipitation are anticipated given changes to dynamics, as well as differences in the

385   responses of individual forest domains to changes in evapotranspiration (Kooperman et al., 2018) and differences in moisture recycling rates (Baker and Spracklen, 2022; Dyer et al., 2017). High recycling rates in the Amazon and Congo would suggest an increase in ET should drive an increase in precipitation, whereas lower rates in the Maritime Continent would result in less direct influence over land, notwithstanding the potential underestimation of Amazon recycling rates in ESMs

390   (Kooperman et al., 2018). Fig. 8 summarises the annual and seasonal changes to rainfall arising from

our plausible global-scale forestation scenario, globally and in the tropical domains. Spatially distributed annual changes in 2095 are shown in Fig. S10.

Figs. 8 and S10 demonstrate the impact on annual precipitation at 2050 and 2095 relative to the No LULCC scenario. We find large increases in precipitation over the Maritime Continent (albeit mostly over the ocean) and decreases in the tropical Pacific relative to No LULCC in Max Forest, and increases and decreases either side of the equator relative to No LULCC in Base, resulting from a northward movement of the Intertropical Convergence Zone (ITCZ) (Fig. 9). There is little to no difference in precipitation over the Northern Hemisphere midlatitudes in either LULCC scenario (Fig. S10), reflecting the limited influence of convective rainfall (where land surface processes can have a direct influence) compared to large-scale frontal processes. The Max Forest scenario does show increases in precipitation of ~ 0.5mm day^{-1} over tropical Africa, Nepal, and parts of South America (Fig S10), though these are not statistically significant at the 95% confidence level. Significant changes in annual precipitation over land were also absent when the signal was decomposed into stratiform and convective components. However, substantial changes are observed in the precipitation signal when it is decomposed into meteorological seasons (Fig. 8). For example, globally, rainfall is higher over forested areas in the Max Forest scenario in northern hemisphere autumn (SON) compared to No LULCC, as well as in the Congo Basin in 2095 in spring (MAM - one of the region's rainy seasons). There are decreases in Max Forest Amazon rainfall in MAM and SON but increases in DJF consistent with a shift in the ITCZ. Amazon rainfall decreases in all scenarios in the fall season (SON) in both 2050 and 2095.

The impact of the Max Forest scenario on annual precipitation over forested areas is not uniform across different regions. Trees are important in the maintenance of intensive tropical precipitation regimes via evapotranspiration and moisture recycling processes (Smith et al., 2023a), but the extent of this influence depends on regional dynamics (Kooperman et al., 2018). The limited ET increase in the Amazon (Fig. 3) limits the local precipitation increase. In the Maritime Continent, ET changes are not significant, which leaves the precipitation signal to be determined by a northward shift of the ITCZ, itself less affected by discontinuities over land in this region compared to the Amazon and Congo (Nicholson, 2018). Over the Congo, the small but statistically significant increases in key parameters such as ET, latent heat flux, and convective cloud cover (sections 3.1 and 3.2) do not linearly translate to a significant annual precipitation increase, likely due to the region's complex dependency on moisture advection from remote sources (e.g. King et al., 2021; Munday et al., 2021) along with recycling (Dyer et al., 2017; Crowhurst et al., 2021). Trees directly influence atmospheric dynamics by increasing the roughness length compared to other, shorter vegetation types. The height at which momentum in a turbulent flow reaches zero is increased by up to 1m in Max Forest relative to No LULCC, most prominently in tropical rainforests where canopy height is greatest (Fig. S7A). Forests thus act as a momentum sink for turbulent flows, and field experiments have shown pressure increases at grassland-forest margins when wind blows from a low-roughness grassland to a high-roughness forest as a result of the slowing effect of the transition to a higher roughness length (Nieveen et al., 2001). While such micrometeorological processes are necessarily highly parameterised in CESM2, it is interesting that our results show small increases in pressure reduced to sea level (SLP), particularly at the margins of the Congo Basin where the Max Forest scenario greatly expands tree cover into previously grassland environments (Fig. S7B). A small increase in surface pressure could potentially oppose increased rainfall drivers by reducing the increase in instability resulting from more evapotranspiration; however, a global model is not expected to be able to resolve these processes in detail (Fosser et al., 2015).

Model experiments with idealised forestation and deforestation scenarios have demonstrated the influence of trees on the general circulation (Portmann et al., 2022), in particular the Hadley cell, the dominant mean-state circulation feature in the tropics (Swann et al., 2012). This provides a mechanism by which land use change can affect climate remotely via teleconnection mechanisms
440   analogous to those that drive the global climate response to internal variability modes such as ENSO (Boysen et al., 2020). Fig. 9 illustrates the response of the Hadley circulation to the Base and Max Forest scenarios with respect to No LULCC by the end of the 21st century. In both scenarios, the response is characterised by a northward displacement of the ascending limb of the circulation with enhanced ascent (negative omega change) and a corresponding increase in descent (positive omega
445   change) immediately south of the Equator. This results from changes to the hemispheric energy gradient due to northern hemisphere warming and ET increases (Laguë et al., 2019, 2021), in which the expected response in SSP1 is enhanced in Max Forest due to additional tree cover. The change here is consistent with the results of Portmann et al. (2022) who also used CESM2 to investigate the impacts of an idealised forestation scenario. However, with our land use change scenario, the
450   magnitude of the change is much smaller. The increasing ascent north of the Equator, associated with forest expansion, is only statistically significant below 900hPa in Base vs No LULCC (Fig. 9); it is both stronger and more significant further into the troposphere (up to 800hPa) in Max Forest vs No LULCC. Fig. 9 thus shows how Max Forest enhances the existing Hadley circulation response from the moderate forest expansion in the SSP1 scenario, with implications for future climate in the tropics
455   including shifts in the locations and seasonality of convection and subsidence.
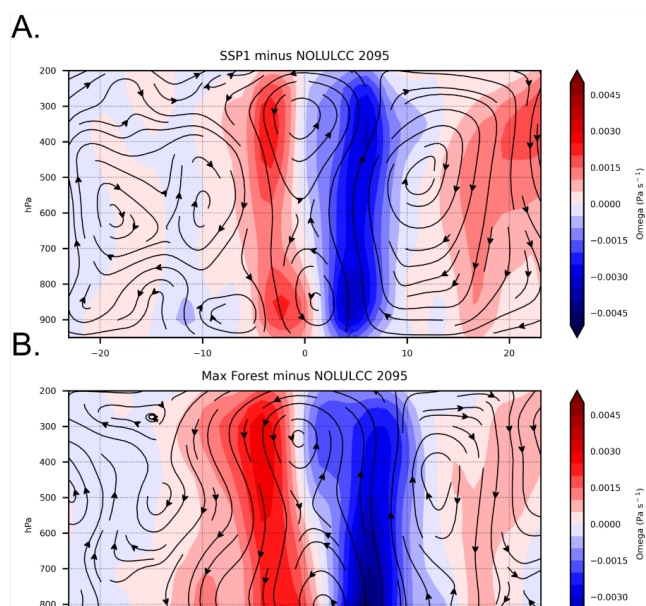
Figure 9 - *differences in the Hadley circulation between scenarios at the end of the 21st century. Contour data is vertical velocity (omega); streamlines are the resultant vectors of omega x 1000 and meridional wind. Data are*
460   *averaged over tropical latitudes.*

4. Discussion

In this study, we apply a global afforestation, reforestation, and forest restoration scenario within a
greenhouse gas concentration scenario which is compatible with the temperature goals of the Paris
Agreement. We demonstrate that, in this scenario, forest expansion increases evapotranspiration and
latent heat flux, while increasing water demand at the land surface and decreasing soil moisture and water
supply as a result. The scenario avoids planting trees on croplands, urban regions and protected
conservation areas; consequently, about 50% of the forest expansion occurs at the expense of grasslands
(Parr et al., 2024) and other non-forest biomes. Since the demands for water and nutrients from trees
are so much greater than those of grasses, especially during the transition from saplings to mature trees
which occurs on the timescales of our model experiments, our results underline the importance of
considering the long-term viability of trees as a climate change mitigation strategy (Hoek van Dijke et al.,
2022). Our scenario attempts only to plant trees in climatically suitable locations, but as we impose land
use change, we do not realistically represent tree mortality or the long-term viability of our expanded
forest areas. This is particularly relevant for forest expansion schemes in the tropics, where most of the
increased tree cover in both the Max Forest scenario and the global restoration commitments is
undertaken. In addition, we do not consider the role of fire in this study, which will have important
implications for future climate and air quality in a warmer world with more trees; evaluating the fire
implications of forest expansion under future climates should be a research priority and will be the focus
of future work.

The viability of global-scale forest expansion will depend upon water availability, among other needs. In
this sense afforestation has greater risks than reforestation and forest restoration, since the increase in
water and nutrient demand is greater. There is a large spread across the CMIP6 ensemble in terms of
simulation of tropical rainfall; while CESM2 is improved in this regard relative to previous versions of the
model (Danabasoglu et al., 2020), and performs well relative to other CMIP6 models (Lee & Wang,
2021), the future trajectory of rainfall in tropical rainforests is still uncertain. For example, while the
CMIP6 ensemble generally projects precipitation increases over the Congo Basin (Dosio et al., 2021) and
decreases over the Amazon (Parsons, 2020) under higher warming scenarios, the ability of models to
simulate present-day tropical rainfall is extremely variable (Dosio et al., 2021), and trends under the
lower SSP1-2.6 scenario used here are small. We note that an increase in the magnitude of the seasonal
cycle of precipitation has been observed in the Amazon in recent decades, with limited interannual change
(Liang et al., 2020) but more extensive droughts (Marengo et al., 2018). Our results indicate that
precipitation increases may result from forest expansion in the Congo Basin, primarily in the spring rainy
season, but that the potential for increased Amazon rainfall in some seasons is not sufficient to counteract
decreases in other seasons; in the case of the Amazon, forest expansion does not prevent the future
tendency towards drying or enhancement of the seasonal precipitation cycle. Model differences in land
surface/atmosphere coupling likely reflect different approaches to parameterising processes at sub-grid
scales (Crowhurst et al., 2020). Our results have important implications for planning reforestation,
afforestation, and forest enhancement because of the water demand increases, and we encourage similar
studies using different Earth System models given the uncertainty in tropical precipitation simulation.
Recent work has shown saturation of global water use efficiency since 2001 (Li et al., 2023) despite
increases in evapotranspiration over the same time period (Yang et al., 2023), which highlights the
importance of considering soil water demands in the terrestrial biosphere from a CDR perspective, and
may limit the future effectiveness of evapotranspiration-driven surface cooling mechanisms. Further, the

increase in total evapotranspiration resulting from forest expansion is constrained by the decreasing soil evaporation resulting from reductions in soil moisture and increased shading of the surface, which act to partially offset increases in transpiration driven by higher NPP (Fig. S9). Combined with the decreases in stomatal conductance due to elevated CO_2 levels in future, which would tend to reduce
510 evapotranspiration, there is not as strong an effect on evapotranspiration from Max Forest as might initially be anticipated from the increases in tropical tree cover (Fig. S9). The stomatal conductance effect would be more pronounced at a higher CO_2 concentration and further work could explore this using other SSP GHG scenarios.

While the Max Forest scenario expands forest area in both the Amazon and the Congo at similar rates, it
515 is in the Congo where the most significant impacts on the land surface and clouds are seen. This is an important result given recent work highlighting the differences in moisture recycling between the two rainforest basins in CMIP6 models (Baker and Spracklen, 2022); generally speaking, models capture moisture recycling in the Congo well, but underestimate it in the Amazon, leading to an under-sensitivity of Amazon climate to LULCC. Our model runs showed large SST variability in the tropical Pacific that
520 may have obscured LULCC-driven changes to the Amazon hydroclimate; while this could be resolved with more ensemble members and/or a multi-model approach, the findings of Baker and Spracklen (2022) suggest this would not fully capture the sensitivity of the Amazonian climate to LULCC. Our results showing changes to cloud cover and convection over the Congo may, therefore, also apply to the Amazon.

There is a balance to be struck when designing experiments to investigate the climate impacts of LULCC
525 between using idealised scenarios to elucidate fundamental processes (Portmann et al., 2022) and scenarios that reflect actual LULCC trends or proposals (Swann et al., 2015). In policy-relevant scenarios, the signals are likely to be smaller given the limited impact of such LULCC in a world where changes to atmospheric dynamics will be dominated by warming, the Clausius-Clapeyron effect, and SST pattern change. Nevertheless, our results do suggest some impact of forest expansion on low cloud cover, which
530 has a negative cloud radiative effect and cools the surface, particularly in the tropics where evaporative cooling also becomes significant. Enhancements in the strength of the tropical circulation might also affect cloud cover over land in Africa. This is in line with the mechanism proposed by Duveiller et al. (2021) based on observations. Additionally, the ability of trees to cool the surface via evapotranspiration is clear in the tropics, but we do not simulate a significant effect in the midlatitudes, which has recently been
535 proposed as a cooling mechanism in the eastern US (Barnes et al., 2024). However, we do not see the impacts on rainfall that might be expected given increased cloud cover and CCN. This result is the reverse of that found by Swann et al. (2015) in a study modelling realistic deforestation in the Amazon. Swann et al. (2015) found that the LULCC influence on rainfall was small because of the already high levels of instability and convective rainfall found in the Amazon. In our model, increases in clouds, cloud water
540 and CCN are only especially significant in tropical rainforests where these quantities are already very high. We encourage the use of high-resolution multi-scale Earth System Modelling, such as the newly developed MUSICA configuration of CESM2 (Pfister et al., 2020), to explore LULCC/climate interactions in more detail, combining high-resolution dynamics and sophisticated atmospheric chemistry in a fully-coupled model. It would also be useful to examine the sensitivity of different convection
545 parameterisations to increased forest cover when combined with chemistry schemes, given the impacts from both increased evapotranspiration and increased CCN that result.

550   5.   Conclusions

We used CESM2 to evaluate the global and regional hydroclimatic impacts of a global forestation scenario. We found a surface cooling due to increased evapotranspiration in the tropics which outweighed albedo-driven warming. No significant temperature effect was found in temperate forestation regions. Plant
555   water demand increased significantly as a result of afforestation which shifted grassland to forest, driving strong decreases in soil moisture across domains as well as decreasing water availability which were not offset by water savings from stomatal closure under the moderate CO2 increases of our scenario. Such changes in water dynamics may pose challenges for regions already susceptible to water scarcity. Additionally, the reduced water availability could impact agriculture and food production, particularly in
560   areas where these sectors rely heavily on groundwater and rivers. In the atmosphere, increases in low cloud were simulated over some, primarily tropical, domains, with a decrease in the magnitude of the cloud radiative effect. Concentrations of cloud condensation nuclei increased over the expanded forests, while small but significant increases in cloud water and convective cloud cover occurred over tropical Africa. However, overall there was little annual precipitation change over land as a result of the LULCC.
565   This was likely due to a combination of factors; the increase in plant transpiration was partially offset by decreasing evaporation from soil; increases in the local drivers of precipitation were small and localised over tropical rainforests, where their magnitude was already very large; the signal from the LULCC was small compared to that from the background warming scenario and SST change; the representation of tropical rainfall and land surface/atmosphere coupling in the model is limited by parameterisation of sub-
570   grid processes; and changes to surface winds from increasing roughness can result in surface pressure increases. We found a northward shift of the Hadley circulation, in line with similar studies using more idealised LULCC, suggesting an impact of forest cover on large scale atmospheric circulation. However, this did not have a significant impact on rainfall over land. Our results suggest that when combined with GHG emissions reductions in a Paris-compatible world, CDR-focused global-scale forest expansion has
575   the potential to deliver substantial climate change mitigation benefits without significantly disrupting global hydroclimate. However, the regional impacts on soil moisture and water availability are of vital importance when planning any kind of forest-based CDR and could hinder climate change mitigation efforts if they are not given sufficient consideration.

580   6.   Code Availability

The CESM2 model code is freely available online and can be downloaded from https://www.cesm.ucar.edu/models. Python scripts used in the preparation of the figures are available from the lead author on request.

585

7.   Data Availability

The output from the CESM2 model experiments used in the analysis, along with the land use change data for each scenario, are freely available at the following repositories: input data (DOI:
590   10.5281/zenodo.10782834), land output data (DOI: 10.5281/zenodo.10797041), atmosphere output data (DOI: 10.5281/zenodo.10797083, 10.5281/zenodo.10797087, 10.5281/zenodo.10797092).

8. Author Contributions

595   JAK and MVM conceived the study with input from JW, PL, and ALSS. PL and SR developed the Max
Forest scenario. JAK designed and performed model experiments, analysed the outputs, and wrote the
original draft. JW, MVM, ALSS, and SR contributed to the development of the manuscript. MVM
provided project funding.

600   9. Competing Interests

JAK sits on an advisory panel for Ecologi, an organization that invests in ecosystem restoration projects.

10. Acknowledgements

605

This project was funded by a United Kingdom Research and Innovation (UKRI) Future Leaders
Fellowship awarded to MVM (grant number MR/T019867/1). ALSS acknowledges support from the US
Department of Energy Office of Biological and Environmental Research Regional and Global Model
Analysis Program (DE-SC0021209). Model experiments were performed on the UK National
610   Supercomputing Service ARCHER2. We thank Wuhu Feng, Chris Symonds, Grenville Lister, and
Michael Mineter for technical support on ARCHER2. Data analysis was performed using JASMIN, the
UK's collaborative data analysis environment. We acknowledge the support of the NCAR Land Model
Working Group (LMWG) and Atmospheric Chemistry Observations and Modelling Group (ACOM).
We also thank Simone Tilmes and Adam Herrington (NCAR), and Daniel Grosvenor (U. Leeds) for
615   helpful comments.

11. References

Abiodun, B. J., Salami, A. T., Matthew, O. J., and Odedokun, S.: Potential impacts of afforestation on
620   climate change and extreme events in Nigeria, Clim. Dyn., 41, 277–293,
https://doi.org/10.1007/S00382-012-1523-9/FIGURES/16, 2013.

Alkama, R. and Cescatti, A.: Climate change: Biophysical climate impacts of recent changes in global
forest cover, Science (80-.)., 351, 600–604,
https://doi.org/10.1126/SCIENCE.AAC8083/SUPPL_FILE/AAC8083-ALKAMA-SM.PDF, 2016.

625   Baker, J. C. A. and Spracklen, D. V.: Divergent Representation of Precipitation Recycling in the
Amazon and the Congo in CMIP6 Models, Geophys. Res. Lett., 49, e2021GL095136,
https://doi.org/10.1029/2021GL095136, 2022.

Barnes, M. L., Zhang, Q., Robeson, S. M., Young, L., Burakowski, E. A., Oishi, A. C., Stoy, P. C.,
Katul, G., and Novick, K. A.: A Century of Reforestation Reduced Anthropogenic Warming in the
630   Eastern United States, Earth's Futur., 12, e2023EF003663, https://doi.org/10.1029/2023EF003663,

2024.

Bastin, J. F., Finegold, Y., Garcia, C., Mollicone, D., Rezende, M., Routh, D., Zohner, C. M., and Crowther, T. W.: The global tree restoration potential, Science (80-.)., 364, 76–79, https://doi.org/10.1126/SCIENCE.AAX0848/SUPPL_FILE/AAX0848_BASTIN_SM_DATA-FILE-S2.CSV, 2019.

Bekenshtein, R., Price, C., and Mareev, E.: Is Amazon deforestation decreasing the number of thunderstorms over South America?, Q. J. R. Meteorol. Soc., https://doi.org/10.1002/QJ.4518, 2023.

Bonan, G. B.: Forests and climate change: forcings, feedbacks, and the climate benefits of forests, Science (80-.)., 320, 1444–1449, https://doi.org/10.1126/science.1155121, 2008.

Bonan, G. B.: Forests, Climate, and Public Policy: A 500-Year Interdisciplinary Odyssey, Annu. Rev. Ecol. Evol. Syst., 47, 97–121, https://doi.org/10.1146/annurev-ecolsys-121415-032359, 2016.

Bonan, G. B., Pollard, D., and Thompson, S. L.: Effects of boreal forest vegetation on global climate, Nat. 1992 3596397, 359, 716–718, https://doi.org/10.1038/359716a0, 1992.

Bond, W. J., Stevens, N., Midgley, G. F., and Lehmann, C. E. R.: The Trouble with Trees: Afforestation Plans for Africa, Trends Ecol. Evol., 34, 963–965, https://doi.org/10.1016/J.TREE.2019.08.003, 2019.

Boysen, L. R., Brovkin, V., Pongratz, J., Lawrence, D. M., Lawrence, P., Vuichard, N., Peylin, P., Liddicoat, S., Hajima, T., Zhang, Y., Rocher, M., Delire, C., Séférian, R., Arora, V. K., Nieradzik, L., Anthoni, P., Thiery, W., Laguë, M. M., Lawrence, D., and Lo, M. H.: Global climate response to idealized deforestation in CMIP6 models, Biogeosciences, 17, 5615–5638, https://doi.org/10.5194/bg-17-5615-2020, 2020.

Chadwick, R., Boutle, I., and Martin, G.: Spatial Patterns of Precipitation Change in CMIP5: Why the Rich Do Not Get Richer in the Tropics, J. Clim., 26, 3803–3822, https://doi.org/10.1175/JCLI-D-12-00543.1, 2013.

Crowhurst, D., Dadson, S., Peng, J., and Washington, R.: Contrasting controls on Congo Basin evaporation at the two rainfall peaks, Clim. Dyn., 56, 1609–1624, https://doi.org/10.1007/S00382-020-05547-1/FIGURES/8, 2021.

Crowhurst, D. M., Dadson, S. J., and Washington, R.: Evaluation of Evaporation Climatology for the Congo Basin Wet Seasons in 11 Global Climate Models, J. Geophys. Res. Atmos., 125, https://doi.org/10.1029/2019JD030619, 2020.

Danabasoglu, G., Bates, S. C., Briegleb, B. P., Jayne, S. R., Jochum, M., Large, W. G., Peacock, S., and Yeager, S. G.: The CCSM4 Ocean Component, J. Clim., 25, 1361–1389, https://doi.org/10.1175/JCLI-D-11-00091.1, 2012.

Danabasoglu, G., Lamarque, J. F., Bacmeister, J., Bailey, D. A., DuVivier, A. K., Edwards, J., Emmons, L. K., Fasullo, J., Garcia, R., Gettelman, A., Hannay, C., Holland, M. M., Large, W. G., Lauritzen, P. H., Lawrence, D. M., Lenaerts, J. T. M., Lindsay, K., Lipscomb, W. H., Mills, M. J., Neale, R., Oleson, K. W., Otto-Bliesner, B., Phillips, A. S., Sacks, W., Tilmes, S., van Kampenhout, L., Vertenstein, M., Bertini, A., Dennis, J., Deser, C., Fischer, C., Fox-Kemper, B., Kay, J. E., Kinnison, D., Kushner, P. J., Larson, V. E., Long, M. C., Mickelson, S., Moore, J. K., Nienhouse, E., Polvani, L., Rasch, P. J., and Strand, W. G.: The Community Earth System Model Version 2 (CESM2), J. Adv. Model. Earth Syst., 12, https://doi.org/10.1029/2019MS001916, 2020.

Dosio, A., Jury, M. W., Almazroui, M., Ashfaq, M., Diallo, I., Engelbrecht, F. A., Klutse, N. A. B.,

Lennard, C., Pinto, I., Sylla, M. B., and Tamoffo, A. T.: Projected future daily characteristics of
675   African precipitation based on global (CMIP5, CMIP6) and regional (CORDEX, CORDEX-CORE)
climate models, Clim. Dyn., 57, 3135–3158, https://doi.org/10.1007/S00382-021-05859-
W/FIGURES/12, 2021.

Drever, C. R., Cook-Patton, S. C., Akhter, F., Badiou, P. H., Chmura, G. L., Davidson, S. J.,
Desjardins, R. L., Dyk, A., Fargione, J. E., Fellows, M., Filewod, B., Hessing-Lewis, M., Jayasundara,
680   S., Keeton, W. S., Kroeger, T., Lark, T. J., Le, E., Leavitt, S. M., LeClerc, M. E., Lemprière, T. C.,
Metsaranta, J., McConkey, B., Neilson, E., St-Laurent, G. P., Puric-Mladenovic, D., Rodrigue, S.,
Soolanayakanahally, R. Y., Spawn, S. A., Strack, M., Smyth, C., Thevathasan, N., Voicu, M.,
Williams, C. A., Woodbury, P. B., Worth, D. E., Xu, Z., Yeo, S., and Kurz, W. A.: Natural climate
solutions for Canada, Sci. Adv., 7, https://doi.org/10.1126/sciadv.abd6034, 2021.

685   Duveiller, G., Filipponi, F., Ceglar, A., Bojanowski, J., Alkama, R., and Cescatti, A.: Revealing the
widespread potential of forests to increase low level cloud cover, Nat. Commun. 2021 121, 12, 1–15,
https://doi.org/10.1038/s41467-021-24551-5, 2021.

Dyer, E. L. E., Jones, D. B. A., Nusbaumer, J., Li, H., Collins, O., Vettoretti, G., and Noone, D.:
Congo Basin precipitation: Assessing seasonality, regional interactions, and sources of moisture, J.
690   Geophys. Res. Atmos., 122, 6882–6898, https://doi.org/10.1002/2016JD026240, 2017.

Emmons, L. K., Schwantes, R. H., Orlando, J. J., Tyndall, G., Kinnison, D., Lamarque, J. F., Marsh,
D., Mills, M. J., Tilmes, S., Bardeen, C., Buchholz, R. R., Conley, A., Gettelman, A., Garcia, R.,
Simpson, I., Blake, D. R., Meinardi, S., and Pétron, G.: The Chemistry Mechanism in the Community
Earth System Model Version 2 (CESM2), J. Adv. Model. Earth Syst., 12, e2019MS001882,
695   https://doi.org/10.1029/2019MS001882, 2020.

Fankhauser, S., Smith, S. M., Allen, M., Axelsson, K., Hale, T., Hepburn, C., Kendall, J. M., Khosla,
R., Lezaun, J., Mitchell-Larson, E., Oberteiner, M., Rajamani, L., Rickaby, R., Seddon, N., and
Wetzer, T.: The meaning of net zero and how to get it right, Nat. Clim. Chang. 2022 121, 12, 15–21,
https://doi.org/10.1038/s41558-021-01245-w, 2021.

700   Fleischman, F., Basant, S., Chhatre, A., Coleman, E. A., Fischer, H. W., Gupta, D., Güneralp, B.,
Kashwan, P., Khatri, D., Muscarella, R., Powers, J. S., Ramprasad, V., Rana, P., Solorzano, C. R.,
and Veldman, J. W.: Pitfalls of Tree Planting Show Why We Need People-Centered Natural Climate
Solutions, Bioscience, 70, 947–950, https://doi.org/10.1093/BIOSCI/BIAA094, 2020.

Fosser, G., Khodayar, S., and Berg, P.: Benefit of convection permitting climate model simulations in
705   the representation of convective precipitation, Clim. Dyn., 44, 45–60,
https://doi.org/10.1007/S00382-014-2242-1/FIGURES/9, 2015.

Friedlingstein, P., Allen, M., Canadell, J. G., Peters, G. P., and Seneviratne, S. I.: Comment on "The
global tree restoration potential," Science (80-.)., 366, 76–79,
https://doi.org/10.1126/science.aay8060, 2019.

710   Fuhrman, J., McJeon, H., Patel, P., Doney, S. C., Shobe, W. M., and Clarens, A. F.: Food–energy–
water implications of negative emissions technologies in a +1.5 °C future, Nat. Clim. Chang., 10, 920–
927, https://doi.org/10.1038/s41558-020-0876-z, 2020.

Gidden, M. J., Riahi, K., Smith, S. J., Fujimori, S., Luderer, G., Kriegler, E., Van Vuuren, D. P., Van
Den Berg, M., Feng, L., Klein, D., Calvin, K., Doelman, J. C., Frank, S., Fricko, O., Harmsen, M.,
715   Hasegawa, T., Havlik, P., Hilaire, J., Hoesly, R., Horing, J., Popp, A., Stehfest, E., and Takahashi, K.:
Global emissions pathways under different socioeconomic scenarios for use in CMIP6: A dataset of
harmonized emissions trajectories through the end of the century, Geosci. Model Dev., 12, 1443–

1475, https://doi.org/10.5194/GMD-12-1443-2019, 2019.

720   Girardin, C. A. J., Jenkins, S., Seddon, N., Allen, M., Lewis, S. L., Wheeler, C. E., Griscom, B. W., and Malhi, Y.: Nature-based solutions can help cool the planet—if we act now, Nature, 593, 191–194, https://doi.org/10.1038/d41586-021-01241-2, 2021.

Grassi, G., House, J., Dentener, F., Federici, S., Den Elzen, M., and Penman, J.: The key role of forests in meeting climate targets requires science for credible mitigation, Nat. Clim. Chang., 7, 220–226, https://doi.org/10.1038/nclimate3227, 2017.

725   Guenther, A. B., Jiang, X., Heald, C. L., Sakulyanontvittaya, T., Duhl, T., Emmons, L. K., and Wang, X.: The model of emissions of gases and aerosols from nature version 2.1 (MEGAN2.1): An extended and updated framework for modeling biogenic emissions, Geosci. Model Dev., 5, 1471–1492, https://doi.org/10.5194/GMD-5-1471-2012, 2012.

Heald, C. L. and Spracklen, D. V.: Land Use Change Impacts on Air Quality and Climate, Chem. Rev.,
730   115, 4476–4496, https://doi.org/10.1021/cr500446g, 2015.

Hoek van Dijke, A. J., Herold, M., Mallick, K., Benedict, I., Machwitz, M., Schlerf, M., Pranindita, A., Theeuwen, J. J. E., Bastin, J. F., and Teuling, A. J.: Shifts in regional water availability due to global tree restoration, Nat. Geosci. 2022 155, 15, 363–368, https://doi.org/10.1038/s41561-022-00935-0, 2022.

735   Hoesly, R. M., Smith, S. J., Feng, L., Klimont, Z., Janssens-Maenhout, G., Pitkanen, T., Seibert, J. J., Vu, L., Andres, R. J., Bolt, R. M., Bond, T. C., Dawidowski, L., Kholod, N., Kurokawa, J. I., Li, M., Liu, L., Lu, Z., Moura, M. C. P., O'Rourke, P. R., and Zhang, Q.: Historical (1750-2014) anthropogenic emissions of reactive gases and aerosols from the Community Emissions Data System (CEDS), Geosci. Model Dev., 11, 369–408, https://doi.org/10.5194/GMD-11-369-2018, 2018.

740   Kennedy, D., Swenson, S., Oleson, K. W., Lawrence, D. M., Fisher, R., Lola da Costa, A. C., and Gentine, P.: Implementing Plant Hydraulics in the Community Land Model, Version 5, J. Adv. Model. Earth Syst., 11, 485–513, https://doi.org/10.1029/2018MS001500, 2019.

King, J. A. and Washington, R.: Future Changes in the Indian Ocean Walker Circulation and Links to Kenyan Rainfall, J. Geophys. Res. Atmos., 126, e2021JD034585,
745   https://doi.org/10.1029/2021JD034585, 2021.

King, J. A., Engelstaedter, S., Washington, R., and Munday, C.: Variability of the Turkana Low-Level Jet in Reanalysis and Models: Implications for Rainfall, J. Geophys. Res. Atmos., 126, e2020JD034154, https://doi.org/10.1029/2020JD034154, 2021.

Kirschbaum, M. U. F., Whitehead, D., Dean, S. M., Beets, P. N., Shepherd, J. D., and Ausseil, A. G.
750   E.: Implications of albedo changes following afforestation on the benefits of forests as carbon sinks, Biogeosciences, 8, 3687–3696, https://doi.org/10.5194/BG-8-3687-2011, 2011.

Kok, M. T. J., Meijer, J. R., van Zeist, W.-J., Hilbers, J. P., Immovilli, M., Janse, J. H., Stehfest, E., Bakkenes, M., Tabeau, A., Schipper, A. M., and Alkemade, R.: Assessing ambitious nature conservation strategies in a below 2-degree and food-secure world, Biol. Conserv., 284, 110068,
755   https://doi.org/10.1016/J.BIOCON.2023.110068, 2023.

Kooperman, G. J., Chen, Y., Hoffman, F. M., Koven, C. D., Lindsay, K., Pritchard, M. S., Swann, A. L. S., and Randerson, J. T.: Forest response to rising CO2 drives zonally asymmetric rainfall change over tropical land, Nat. Clim. Chang. 2018 85, 8, 434–440, https://doi.org/10.1038/s41558-018-0144-7, 2018.

760   Laguë, M. M., Bonan, G. B., and Swann, A. L. S.: Separating the Impact of Individual Land Surface

Properties on the Terrestrial Surface Energy Budget in both the Coupled and Uncoupled Land–Atmosphere System, J. Clim., 32, 5725–5744, https://doi.org/10.1175/JCLI-D-18-0812.1, 2019.

Laguë, M. M., Swann, A. L. S., and Boos, W. R.: Radiative Feedbacks on Land Surface Change and Associated Tropical Precipitation Shifts, J. Clim., 34, 6651–6672, https://doi.org/10.1175/JCLI-D-20-0883.1, 2021.

Lawrence, D., Coe, M., Walker, W., Verchot, L., and Vandecar, K.: The Unseen Effects of Deforestation: Biophysical Effects on Climate, Front. For. Glob. Chang., 5, 756115, https://doi.org/10.3389/FFGC.2022.756115/BIBTEX, 2022.

Lawrence, D. M., Hurtt, G. C., Arneth, A., Brovkin, V., Calvin, K. V., Jones, A. D., Jones, C. D., Lawrence, P. J., Noblet-Ducoudré, N. De, Pongratz, J., Seneviratne, S. I., and Shevliakova, E.: The Land Use Model Intercomparison Project (LUMIP) contribution to CMIP6: Rationale and experimental design, Geosci. Model Dev., 9, 2973–2998, https://doi.org/10.5194/GMD-9-2973-2016, 2016.

Lawrence, D. M., Fisher, R. A., Koven, C. D., Oleson, K. W., Swenson, S. C., Bonan, G., Collier, N., Ghimire, B., van Kampenhout, L., Kennedy, D., Kluzek, E., Lawrence, P. J., Li, F., Li, H., Lombardozzi, D., Riley, W. J., Sacks, W. J., Shi, M., Vertenstein, M., Wieder, W. R., Xu, C., Ali, A. A., Badger, A. M., Bisht, G., van den Broeke, M., Brunke, M. A., Burns, S. P., Buzan, J., Clark, M., Craig, A., Dahlin, K., Drewniak, B., Fisher, J. B., Flanner, M., Fox, A. M., Gentine, P., Hoffman, F., Keppel-Aleks, G., Knox, R., Kumar, S., Lenaerts, J., Leung, L. R., Lipscomb, W. H., Lu, Y., Pandey, A., Pelletier, J. D., Perket, J., Randerson, J. T., Ricciuto, D. M., Sanderson, B. M., Slater, A., Subin, Z. M., Tang, J., Thomas, R. Q., Val Martin, M., and Zeng, X.: The Community Land Model Version 5: Description of New Features, Benchmarking, and Impact of Forcing Uncertainty, J. Adv. Model. Earth Syst., 11, 4245–4287, https://doi.org/10.1029/2018MS001583, 2019.

Lawrence, M. G., Schäfer, S., Muri, H., Scott, V., Oschlies, A., Vaughan, N. E., Boucher, O., Schmidt, H., Haywood, J., and Scheffran, J.: Evaluating climate geoengineering proposals in the context of the Paris Agreement temperature goals, Nat. Commun. 2018 91, 9, 1–19, https://doi.org/10.1038/s41467-018-05938-3, 2018.

Lee, T.-H., Lo, M.-H., Chiang, C.-L., and Kuo, Y.-N.: The maritime continent's rainforests modulate the local interannual evapotranspiration variability, Commun. Earth Environ. 2023 41, 4, 1–7, https://doi.org/10.1038/s43247-023-01126-4, 2023.

Lee, Y. C. and Wang, Y. C.: Evaluating diurnal rainfall signal performance from cmip5 to cmip6, J. Clim., 34, 7607–7623, https://doi.org/10.1175/JCLI-D-20-0812.1, 2021.

Lewis, S. L., Mitchard, E. T. A., Prentice, C., Maslin, M., and Poulter, B.: Comment on "The global tree restoration potential," Science (80-.)., 366, 1–3, https://doi.org/10.1126/SCIENCE.AAZ0388, 2019a.

Lewis, S. L., Wheeler, C. E., Mitchard, E. T. A., and Koch, A.: Restoring natural forests is the best way to remove atmospheric carbon, Nature, 568, 25–28, https://doi.org/10.1038/d41586-019-01026-8, 2019b.

Li, F., Xiao, J., Chen, J., Ballantyne, A., Jin, K., Li, B., Abraha, M., and John, R.: Global water use efficiency saturation due to increased vapor pressure deficit, Science, 381, 672–677, https://doi.org/10.1126/SCIENCE.ADF5041/SUPPL_FILE/SCIENCE.ADF5041_SM.PDF, 2023.

Liang, Y. C., Lo, M. H., Lan, C. W., Seo, H., Ummenhofer, C. C., Yeager, S., Wu, R. J., and Steffen, J. D.: Amplified seasonal cycle in hydroclimate over the Amazon river basin and its plume region, Nat. Commun. 2020 111, 11, 1–11, https://doi.org/10.1038/s41467-020-18187-0, 2020.

805   Liu, X., Ma, P. L., Wang, H., Tilmes, S., Singh, B., Easter, R. C., Ghan, S. J., and Rasch, P. J.:
Description and evaluation of a new four-mode version of the Modal Aerosol Module (MAM4) within
version 5.3 of the Community Atmosphere Model, Geosci. Model Dev., 9, 505–522,
https://doi.org/10.5194/GMD-9-505-2016, 2016.

Marengo, J. A., Souza, C. M., Thonicke, K., Burton, C., Halladay, K., Betts, R. A., Alves, L. M., and
810   Soares, W. R.: Changes in Climate and Land Use Over the Amazon Region: Current and Future
Variability and Trends, Front. Earth Sci., 6, 425317,
https://doi.org/10.3389/FEART.2018.00228/BIBTEX, 2018.

Martin, M. P., Woodbury, D. J., Doroski, D. A., Nagele, E., Storace, M., Cook-Patton, S. C.,
Pasternack, R., and Ashton, M. S.: People plant trees for utility more often than for biodiversity or
815   carbon, Biol. Conserv., 261, 109224, https://doi.org/10.1016/J.BIOCON.2021.109224, 2021.

Munday, C., Washington, R., and Hart, N.: African Low-Level Jets and Their Importance for Water
Vapor Transport and Rainfall, Geophys. Res. Lett., 48, e2020GL090999,
https://doi.org/10.1029/2020GL090999, 2021.

Nabuurs, G.-J. and R. Mrabet, A. Abu Hatab, M. Bustamante, H. Clark, P. Havlík, J. House, C.
820   Mbow, K.N. Ninan, A. Popp, S. Roe, B. Sohngen, S. T.: IPCC Mitigation: Agriculture, Forestry and
Other Land Uses, Clim. Chang. 2022 - Mitig. Clim. Chang., 747–860,
https://doi.org/10.1017/9781009157926.009, 2023.

Nicholson, S. E.: The ITCZ and the Seasonal Cycle over Equatorial Africa, Bull. Am. Meteorol. Soc.,
99, 337–348, https://doi.org/10.1175/BAMS-D-16-0287.1, 2018.

825   Nieveen, J. P., El-Kilani, R. M. M., and Jacobs, A. F. G.: Behaviour of the static pressure around a
tussock grassland–forest interface, Agric. For. Meteorol., 106, 253–259,
https://doi.org/10.1016/S0168-1923(00)00234-3, 2001.

Nosetto, M. D., Jobbágy, E. G., and Paruelo, J. M.: Land-use change and water losses: the case of
grassland afforestation across a soil textural gradient in central Argentina, Glob. Chang. Biol., 11,
830   1101–1117, https://doi.org/10.1111/J.1365-2486.2005.00975.X, 2005.

Orlov, A., Aunan, K., Mistry, M. N., Lejeune, Q., Pongratz, J., Thiery, W., Gasparrini, A., Reed, E.
U., and Schleussner, C. F.: Neglected implications of land-use and land-cover changes on the climate-
health nexus, Environ. Res. Lett., 18, 061005, https://doi.org/10.1088/1748-9326/ACD799, 2023.

Parr, C. L., Beest, M. te, and Stevens, N.: Conflation of reforestation with restoration is widespread,
835   Science (80-.)., 383, 698–701, https://doi.org/10.1126/SCIENCE.ADJ0899, 2024.

Parsons, L. A.: Implications of CMIP6 Projected Drying Trends for 21st Century Amazonian Drought
Risk, Earth's Futur., 8, e2020EF001608, https://doi.org/10.1029/2020EF001608, 2020.

Pfister, G. G., Eastham, S. D., Arellano, A. F., Aumont, B., Barsanti, K. C., Barth, M. C., Conley,
A., Davis, N. A., Emmons, L. K., Fast, J. D., Fiore, A. M., Gaubert, B., Goldhaber, S., Granier, C.,
840   Grell, G. A., Guevara, M., Henze, D. K., Hodzic, A., Liu, X., Marsh, D. R., Orlando, J. J., Plane, J.
M. C., Polvani, L. M., Rosenlof, K. H., Steiner, A. L., Jacob, D. J., and Brasseur, G. P.: The Multi-
Scale Infrastructure for Chemistry and Aerosols (MUSICA), Bull. Am. Meteorol. Soc., 101, E1743–
E1760, https://doi.org/10.1175/BAMS-D-19-0331.1, 2020.

Portmann, R., Beyerle, U., Davin, E., Fischer, E. M., De Hertog, S., and Schemm, S.: Global
845   forestation and deforestation affect remote climate via adjusted atmosphere and ocean circulation, Nat.
Commun. 2022 131, 13, 1–11, https://doi.org/10.1038/s41467-022-33279-9, 2022.

Robinson, M. and Shine, T.: Achieving a climate justice pathway to 1.5 °C, Nat. Clim. Chang., 8, 564–

569, https://doi.org/10.1038/s41558-018-0189-7, 2018.

850 Roe, S., Streck, C., Obersteiner, M., Frank, S., Griscom, B., Drouet, L., Fricko, O., Gusti, M., Harris, N., Hasegawa, T., Hausfather, Z., Havlík, P., House, J., Nabuurs, G. J., Popp, A., Sánchez, M. J. S., Sanderman, J., Smith, P., Stehfest, E., and Lawrence, D.: Contribution of the land sector to a 1.5 °C world, Nat. Clim. Chang. 2019 911, 9, 817–828, https://doi.org/10.1038/s41558-019-0591-9, 2019.

855 Roe, S., Streck, C., Beach, R., Busch, J., Chapman, M., Daioglou, V., Deppermann, A., Doelman, J., Emmet-Booth, J., Engelmann, J., Fricko, O., Frischmann, C., Funk, J., Grassi, G., Griscom, B., Havlik, P., Hanssen, S., Humpenöder, F., Landholm, D., Lomax, G., Lehmann, J., Mesnildrey, L., Nabuurs, G. J., Popp, A., Rivard, C., Sanderman, J., Sohngen, B., Smith, P., Stehfest, E., Woolf, D., and Lawrence, D.: Land-based measures to mitigate climate change: Potential and feasibility by country, Glob. Chang. Biol., 27, 6025–6058, https://doi.org/10.1111/GCB.15873, 2021a.

860 Roe, S., Lawrence, P. J., Sewell, A., Giesen, P., and Lawrence, D.: Mitigation potential of afforestation, reforestation and forest enhancement, considering impacts from climate change, agricultural expansion, and biodiversity prioritization, Glob. Chang. Biol., 2021b.

Seddon, N., Chausson, A., Berry, P., Girardin, C. A. J., Smith, A., and Turner, B.: Understanding the value and limits of nature-based solutions to climate change and other global challenges, Philos. Trans.
865 R. Soc. B Biol. Sci., 375, https://doi.org/10.1098/rstb.2019.0120, 2020.

Seddon, N., Smith, A., Smith, P., Key, I., Chausson, A., Girardin, C., House, J., Srivastava, S., and Turner, B.: Getting the message right on nature-based solutions to climate change, Glob. Chang. Biol., 27, 1518–1546, https://doi.org/10.1111/gcb.15513, 2021.

Sewell, A., Van Der Esch, S., and Löwenhardt, H.: Goals and Commitments for the Restoration
870 decade: A Global Overview of Countries' Restoration Commitments Under the Rio Conventions and Other Pledges, 1–38, 2020.

Šimpraga, M., Ghimire, R. P., Van Der Straeten, D., Blande, J. D., Kasurinen, A., Sorvari, J., Holopainen, T., Adriaenssens, S., Holopainen, J. K., and Kivimäenpää, M.: Unravelling the functions of biogenic volatiles in boreal and temperate forest ecosystems, Eur. J. For. Res., 138, 763–787,
875 https://doi.org/10.1007/s10342-019-01213-2, 2019.

Sindelarova, K., Granier, C., Bouarar, I., Guenther, A., Tilmes, S., Stavrakou, T., Müller, J. F., Kuhn, U., Stefani, P., and Knorr, W.: Global data set of biogenic VOC emissions calculated by the MEGAN model over the last 30 years, Atmos. Chem. Phys., 14, 9317–9341, https://doi.org/10.5194/ACP-14-9317-2014, 2014.

880 Smith, C., Baker, J. C. A., and Spracklen, D. V.: Tropical deforestation causes large reductions in observed precipitation, Nat. 2023, 1–6, https://doi.org/10.1038/s41586-022-05690-1, 2023a.

Smith, S. M., Geden, O., Nemet, G. F., Gidden, M. J., Lamb, W. F., Powis, C., Bellamy, R., Callaghan, M. W., Cowie, A., Cox, E., Fuss, S., Gasser, T., Grassi, G., Greene, J., Lück, S., Mohan, A., Müller-Hansen, F., Peters, G. P., Pratama, Y., Repke, T., Riahi, K., Schenuit, F., Steinhauser, J.,
885 Strefler, J., Valenzuela, J. M., and Minx, J. C.: The State of Carbon Dioxide Removal - 1st Edition, The State of Carbon Dioxide Removal, https://doi.org/10.17605/OSF.IO/W3B4Z, 2023b.

Sporre, M. K., Blichner, S. M., Karset, I. H. H., Makkonen, R., and Berntsen, T. K.: BVOC-aerosol-climate feedbacks investigated using NorESM, Atmos. Chem. Phys., 19, 4763–4782, https://doi.org/10.5194/acp-19-4763-2019, 2019.

890 Swann, A. L. S., Fung, I. Y., and Chiang, J. C. H.: Mid-latitude afforestation shifts general circulation

and tropical precipitation, Proc. Natl. Acad. Sci. U. S. A., 109, 712–716, https://doi.org/10.1073/PNAS.1116706108/SUPPL_FILE/PNAS.1116706108_SI.PDF, 2012.

Swann, A. L. S., Longo, M., Knox, R. G., Lee, E., and Moorcroft, P. R.: Future deforestation in the Amazon and consequences for South American climate, Agric. For. Meteorol., 214–215, 12–24,
895 https://doi.org/10.1016/j.agrformet.2015.07.006, 2015a.

Swann, A. L. S., Longo, M., Knox, R. G., Lee, E., and Moorcroft, P. R.: Future deforestation in the Amazon and consequences for South American climate, Agric. For. Meteorol., 214–215, 12–24, https://doi.org/10.1016/J.AGRFORMET.2015.07.006, 2015b.

Tai, A. P. K., Martin, M. V., and Heald, C. L.: Threat to future global food security from climate
900 change and ozone air pollution, Nat. Clim. Chang. 2014 49, 4, 817–821, https://doi.org/10.1038/nclimate2317, 2014.

Percent Changes: https://www2.census.gov/programs-surveys/acs/tech_docs/accuracy/percchg.pdf, last access: 23 October 2023.

Val Martin, M., Heald, C. L., Lamarque, J. F., Tilmes, S., Emmons, L. K., and Schichtel, B. A.: How
905 emissions, climate, and land use change will impact mid-century air quality over the United States: A focus on effects at national parks, Atmos. Chem. Phys., 15, 2805–2823, https://doi.org/10.5194/acp-15-2805-2015, 2015.

Wang, J., Chagnon, F. J. F., Williams, E. R., Betts, A. K., Renno, N. O., Machado, L. A. T., Bisht, G., Knox, R., and Bras, R. L.: Impact of deforestation in the Amazon basin on cloud climatology, Proc.
910 Natl. Acad. Sci. U. S. A., 106, 3670–3674, https://doi.org/10.1073/PNAS.0810156106, 2009.

Weber, J., Archer-Nicholls, S., Abraham, N. L., Shin, Y. M., Griffiths, P., Grosvenor, D. P., Scott, C. E., and Archibald, A. T.: Chemistry-driven changes strongly influence climate forcing from vegetation emissions, Nat. Commun. 2022 131, 13, 1–12, https://doi.org/10.1038/s41467-022-34944-9, 2022.

915 Weber, J., King, J. A., Abraham, N. L., Grosvenor, D. P., Smith, C. J., Shin, Y. M., Lawrence, P., Roe, S., Beerling, D. J., and Martin, M. V.: Chemistry-albedo feedbacks offset up to a third of forestation's CO_2 removal benefits, Science (80-.)., 383, 860–864, https://doi.org/10.1126/SCIENCE.ADG6196, 2024.

Whittaker, R. H.: Communities and Ecosystems, 2nd Editio., MacMillan, New York, 1975.

920 Windisch, M. G., Davin, E. L., and Seneviratne, S. I.: Prioritizing forestation based on biogeochemical and local biogeophysical impacts, Nat. Clim. Chang. 2021 1110, 11, 867–871, https://doi.org/10.1038/s41558-021-01161-z, 2021.

De Wit, H. A., Bryn, A., Hofgaard, A., Karstensen, J., Kvalevåg, M. M., and Peters, G. P.: Climate warming feedback from mountain birch forest expansion: reduced albedo dominates carbon uptake,
925 Glob. Chang. Biol., 20, 2344–2355, https://doi.org/10.1111/GCB.12483, 2014.

Yang, Y., Roderick, M. L., Guo, H., Miralles, D. G., Zhang, L., Fatichi, S., Luo, X., Zhang, Y., McVicar, T. R., Tu, Z., Keenan, T. F., Fisher, J. B., Gan, R., Zhang, X., Piao, S., Zhang, B., and Yang, D.: Evapotranspiration on a greening Earth, Nat. Rev. Earth Environ. 2023, 1–16, https://doi.org/10.1038/s43017-023-00464-3, 2023.

930 Zhang, H., Li, L., Song, J., Akhter, Z. H., and Zhang, J.: Understanding aerosol–climate–ecosystem interactions and the implications for terrestrial carbon sink using the Community Earth System Model, Agric. For. Meteorol., 340, 109625, https://doi.org/10.1016/J.AGRFORMET.2023.109625, 2023.

Zickfeld, K., MacIsaac, A. J., Canadell, J. G., Fuss, S., Jackson, R. B., Jones, C. D., Lohila, A., Matthews, H. D., Peters, G. P., Rogelj, J., and Zaehle, S.: Net-zero approaches must consider Earth
935   system impacts to achieve climate goals, Nat. Clim. Chang. 2023 1312, 13, 1298–1305, https://doi.org/10.1038/s41558-023-01862-7, 2023.